JACS
JOURNAL OF THE AMERICAN CHEMICAL SOCIETY
pubs.acs.org/JACS
Article

Zn(II)−Siloxane Clusters as Versatile Building Blocks for Carboxylate-Based Metal−Organic Frameworks

Hyungphil Chun* and Dohyun Moon*

Cite This: J. Am. Chem. Soc. 2023, 145, 18598−18606
Read Online

ABSTRACT: Siloxanes have long been known for their highly desirable properties suited for a wide range of practical applications; however, their utilization as modular building blocks for crystalline open frameworks has been limited. In this study, a simple solvothermal pathway has been found to synthesize unprecedented Zn(II)−siloxane clusters supported by acetate ligands, $[(RSiO_2)_8Zn_8(CH_3CO_2)_8]$ (R = Me or Ph). The same reaction using a dicarboxylate ligand such as 1,4-benzenedicarboxylate or 2,6-naphthalenedicarboxylate produces a new type of metal−organic framework, named SiMOF here, based on the $[Si_8Zn_8]$ units. With the maximum connectivity of 8, the building block is shown to form topologically interesting structures such as octahedral supercages or uninodal 8-connected frameworks. All SiMOFs synthesized possess permanent porosity and high thermal stability and are naturally hydrophobic, as demonstrated by adsorptions of toluene, ethanol, methanol, and water vapor as well as water contact angle measurements. These promising characteristics for well-defined porous solids are attributed to metal-bound siloxane groups in the structural building units.

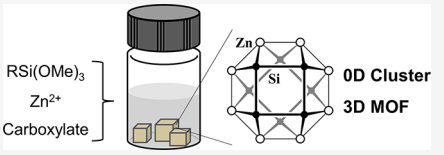

INTRODUCTION

Organosilicon compounds carrying siloxane (Si−O−Si) linkages constitute a very important class of materials because of the highly desirable properties they possess, such as thermal stability, chemical resistance, structural flexibility, low toxicity, etc.[1] From amorphous forms such as silicone oil typified by polydimethylsiloxane[2] to ordered mesoporous structures,[3,4] their commercial and industrial applications cover extremely broad areas. Among various precursors for such organosilicate materials, a monosubstituted silane with three leaving groups ($RSiX_3$) is particularly intriguing because three silanol groups of the hydrolyzed intermediate $[RSi(OH)_3]$ can not only undergo condensation reactions into oligomeric or polymeric siloxanes but also coordinate to metal ions forming metal−siloxane clusters (Scheme 1).

Scheme 1. Conceptual Process Requiring Three Silanol Groups to Form Metal−Siloxane Clusters

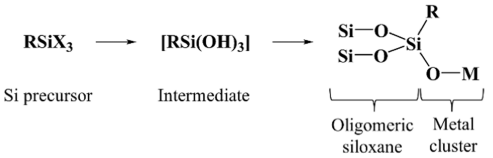

The presence of metal ions in organosilicate materials would be advantageous in view of both structural and functional aspects. Therefore, it is not surprising that molecular clusters of metal-bound cyclic siloxanes have been reported at least 35 years ago[5] and have been an active area of research since then.[6−11] It would be informative to note here that a dominant proportion of these metal−siloxane clusters are of the structural type where transition metal ions are sandwiched between two cyclic siloxanes.[12−15] Despite the persistent coordination behavior of cyclic siloxanes toward s-, d-, and f-block metal ions,[16−18] this area of research has not seen extended solids based on these promising building blocks. This realization naturally leads to the question as to whether the structural chemistry of metal−siloxane can reach beyond the molecular level, which is 0-dimension (0D). The question becomes more relevant and significant when it is considered that one of the most important developments in chemistry research during the last two decades involves coordination-based network solids known as metal−organic frameworks (MOFs). In fact, introducing siloxane building blocks into MOF structures has been a topic of interest until recently. However, studies published in this context have utilized siloxanes as a part of carboxylate ligands,[19] as a coating for MOF crystals[20] or as intercalating materials for hybrid solids,[21] and no report of molecular siloxane building blocks is found in MOF research.

It may not be a coincidence that some of the most impactful MOFs discovered to date are based on simple, readily available linkers such as 1,4-benzenedicarboxylate (MOF-5,[22] UiO-66[23]), 1,3,5-benzenetricarboxylate (HKUST-1,[24] MIL-101[25]), or imidazolates (ZIFs),[26,27] while their metal or metal cluster

Received: June 11, 2023
Published: August 8, 2023

https://doi.org/10.1021/jacs.3c05950
J. Am. Chem. Soc. 2023, 145, 18598−18606

units display a much greater diversity, for example, $[Zn_4O]$, $[Zr_6O_4(OH)_4]$, $[Cu_2]$, $[Cr_3O]$, and [Zn], respectively. This oversimplified view of some of the seminal developments in MOF research has prompted one of the authors to pursue a method to utilize metal−siloxane clusters as potential building blocks for crystalline porous materials.

If connected by simple dicarboxylate linkers, the clusters would become a new type of secondary building units (SBUs) for organosilicate- or siloxane-based framework solids, SiMOFs. Other than the obvious reason that such MOFs based on RSi−O−M linkages are virtually absent in the literature, SiMOFs are attractive targets for synthetic endeavors because the frameworks may inherit, at least partially, the desirable stability of siloxanes suited for practical applications. Also, the combination of numerous carboxylate linkers and unprecedented SBUs of the general composition $(RSiO_2)_xM_y$ would further enrich and deepen the understanding of MOF structures and properties. Finally, siloxanes are often considered as structural models for various building units of silicate minerals including zeolites,[28] for example, polyhedral oligomeric silsesquioxanes mimicking the geometry of double n-rings found in various aluminosilicates.[29−33] Therefore, synthetic efforts toward geometrically diverse metal−siloxane SBUs may ultimately lead to hybrid materials in which building units of MOFs and zeolites are joined at the molecular level and not as a bulk composite.[34,35]

For this initiative study, we used simple ligands, such as acetate or linear dicarboxylates, to support the core unit of Zn(II)-bound cyclic siloxane ($[Si_4Zn_8Si_4]$) and obtained 0D molecular clusters and 3D frameworks, all by simple solvothermal reactions (Scheme 2).

Scheme 2. Line Drawing of a $[Si_4Zn_8Si_4]$ Cluster Supported by Carboxylate Ligands and the List of Compounds Synthesized in This Work

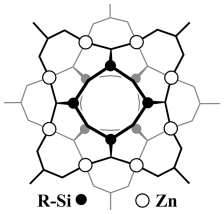

R	Carboxylate	Product
Me	OAc	**1**
Ph	OAc	**2**
Me	1,4-bdc	**SiMOF-11**
Me	2,6-ndc	**SiMOF-12**
Ph	1,4-bdc	**SiMOF-21**

The carboxylate-supported $[Si_8Zn_8]$ unit common in all of the structures has not been documented previously. The general method by which carboxylate-based SiMOFs can be synthesized and the characterization of molecular clusters and three new frameworks are described below.

RESULTS AND DISCUSSION

Most of the known metal−siloxane clusters are synthesized by more or less the same methods adapted from the original publication.[5] In the process, alkali hydroxide is used in an organic solvent to remove alkoxy groups of the Si precursor under a reflux condition, and in the second step, the obtained solid or solution mixture reacts with transition metal and auxiliary ligands, if necessary. The reaction medium in this procedure, however, is found to be too basic to be used for carboxylate linkers, and the two-step reactions are not highly efficient for the fast screening of MOFs having a new composition. Therefore, we attempted a simple solvothermal pathway in which a Si precursor, a Zn^{2+} ion, and carboxylate ligands are allowed to react simultaneously without undergoing unwanted gelation or polymerization. In our methods established by systematically optimizing various reaction parameters, $RSi(OMe)_3$ (R = Me or Ph) dissolved in absolute ethanol is partially hydrolyzed in situ in the presence of $[Zn(OH_2)_6]^{2+}$, and the mixture is heated along with acetic acid under solvothermal conditions. In these methods, other types of Si precursors, such as $RSiCl_3$ or $RSi(OAc)_3$, can also be used; however, all reactions have been optimized using trialkoxysilanes because of their low toxicity and wide availability. The finding that $RSi(OMe)_3$ can be hydrolyzed in a controlled manner without adding water or hydroxides is the essence of this simple and efficient method. The formation of unwanted byproducts from this reaction can be controlled by adding a small amount of DMF and/or weak base such as triethylamine or pyridine, and the acetate-supported clusters $[(RSiO_2)_8Zn_8(OAc)_8]$ (R = Me for **1** and Ph for **2**) are obtained as highly pure crystalline solids. The molecular cluster **1** crystallizes as tetragonal or orthorhombic polymorphs depending on a subtle difference in reaction conditions, while only a cubic phase is obtained for **2** (Figure 1). The tetragonal phase of **1** is identical to the orthorhombic polymorph and is shown in Figure S1. The experimental X-ray powder diffraction (XRPD) patterns of all compounds well-match their simulations based on single-crystal data, proving the bulk purity of the products (Figure 2).

In the structure, each of the terminal O atoms of the cyclic tetramer $[(MeSiO_2)_4]^{4-}$ are bonded to two Zn(II) ions, which are bridged by an acetate ligand. Therefore, the entire cluster is charge-neutral, and all of the Zn(II) ions adopt a tetrahedral coordination geometry. As shown in Figure 1c, the geometrical features of the core unit $[(SiO_2)_8Zn_8]$ for **1** and **2** are almost identical, and the only notable difference is the binding angle of some acetate groups. An almost identical type of $[Si_8Co_8]$ cage has been reported previously by Liu et al.;[9] however, the Co−

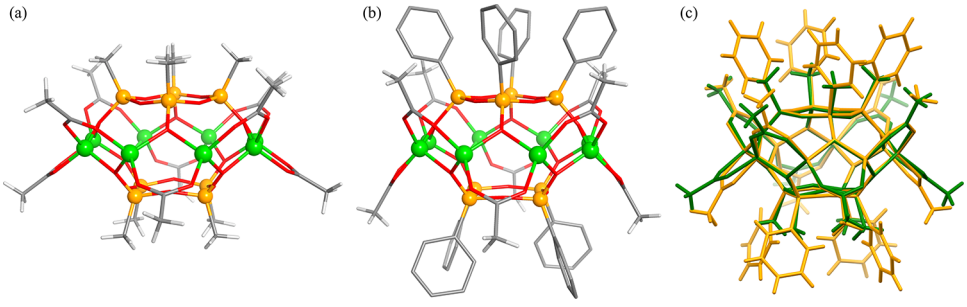

Figure 1. X-ray structures for the molecules **1** (a) and **2** (b). Some H atoms of **2** are omitted for clarity. Color code: green, Zn; orange, Si; red, O; gray, C; and white, H. (c) Molecules **1** and **2** overlaid with Zn atoms on opposite sides as pivot points.

https://doi.org/10.1021/jacs.3c05950
J. Am. Chem. Soc. 2023, 145, 18598−18606

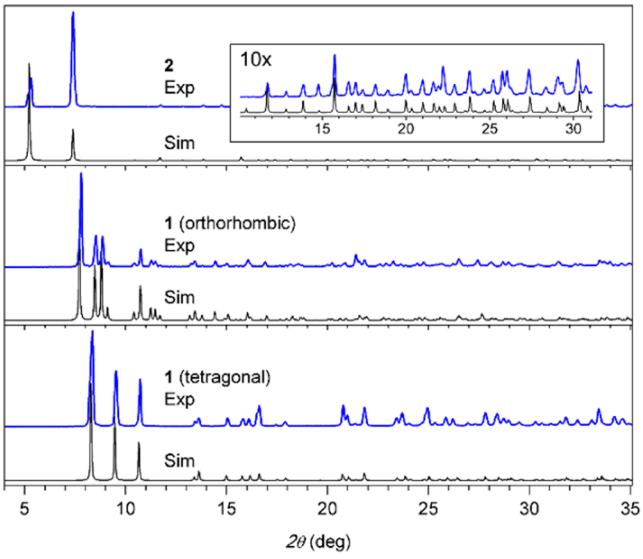

Figure 2. Simulated and experimental XRPD patterns of **1** and **2**; λ = 1.54 Å.

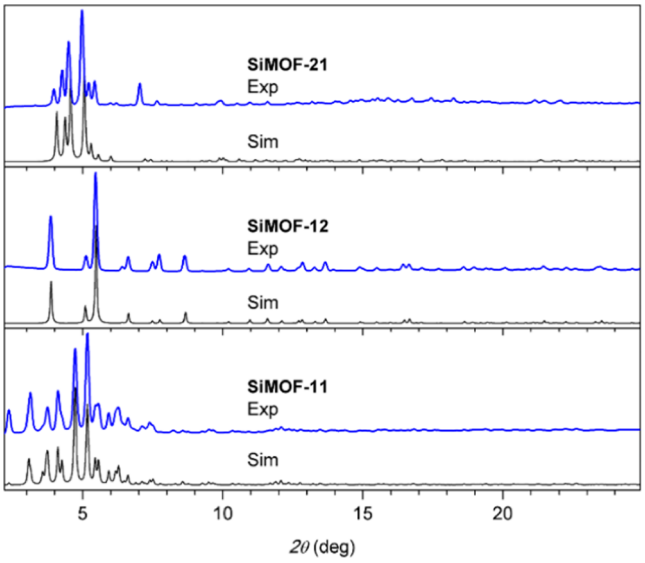

Figure 3. Simulated and experimental XRPD patterns for SiMOFs; λ = 1.20 Å.

siloxane cluster is supported by pyrazolate ligands. To the best of our knowledge, there is no known case of a metal−siloxane cluster supported only by carboxylate ligands.

Topologically, 8 acetate ligands in **1** and **2** render the cluster as a potential 8-connecting SBU with a square antiprism geometry. It is interesting that a vertex- and edge-transitive (11rs) 8-c net with the coordination figure of square antiprism does not exist in the RCSR database.[36] Therefore, any synthetic strategy utilizing the $[Si_8Zn_8]$ cluster for a 3-periodic net would have to diversify either the vertex (SBU) or the edge (organic linker).

The derivation of SiMOFs from the $[Si_8Zn_8]$ cluster with dicarboxylate ligands using the synthetic protocols developed for **1** and **2** was not straightforward until it was realized that the organic linker should be added in the form of an ester, not as a free acid. This is to prevent Zn(II) from forming a polymeric structure with dicarboxylate alone before binding to O atoms of siloxane and also to slow down the overall process through in situ hydrolysis of esters for better crystallization. Other than this minor but crucial modification, solvothermal conditions used in this work are very similar in all cases, and all of the products are obtained as highly crystalline solids with good yields. The three frameworks synthesized here are labeled **SiMOF-11**, **-12**, and **-21** (see below). The experimental XRPD patterns compared to simulations based on single-crystal data prove bulk purities of all SiMOF solids (Figure 3).

The first framework we describe is **SiMOF-11** where the substituent on Si is a methyl group and the linker is 1,4-benzenedicarboxylate (bdc). The structural analysis by single-crystal diffraction reveals some extraordinary features. First, it has a very large unit cell with a volume of 260,000 Å^3 in the $R\bar{3}m$ space group ($a = b$ = 66.8 and c = 67.2 Å), and still, the single-crystal diffractions are observed up to 0.75 Å resolution, implying an exceptional ordering of the crystal lattice.

It is noteworthy that, according to statistical analysis, only 12 single-crystal structures are known from 28,729 entries in the 3D MOF subset of the Cambridge Structural Database (CSD) with the unit cell volume greater than that of **SiMOF-11**,[37] and they are all invariably cubic systems (Table S1). In fact, **SiMOF-11** has the largest unit cell volume for a noncubic space group in the entire MOF subset of CSD, which includes 119,927 structures.[38] Because of its size, the crystallographic asymmetric unit contains 232 non-hydrogen atoms, and overall, 90 $[Si_8Zn_8]$ clusters are present in the unit cell. Second, the framework is built upon 5 independent $[Si_8Zn_8]$ clusters or SBUs interconnected by bdc linkers. We found only one case in the literature where an MOF is composed of 5 SBUs.[39] As shown in Figure 4, the SBUs labeled I−V are different in the number and orientation of bdc ligands replacing the acetate groups in **1**. Thus, the structural formula for **SiMOF-11** established by X-ray analysis is $[(MeSiO_2)_8Zn_8(bdc)_{2.8}(OAc)_{2.4}]$.

Of the 5 SBUs, I−IV assemble to form 3 different supercages (A−C) of octahedral geometry. The distances between two opposite nodes in these octahedra are well over 2 nm. SBU V has only two bdc linkers and bridges between C cages, which are built solely from SBU IV. All 6 vertices of octahedral cage A are shared by cage B so that A and B become the node and edge, respectively, of a **pcu**-like net. Supercage C acts as the node of another **pcu** net that interpenetrates the first one (Figure 4). The last key feature of **SiMOF-11** is that each of the octahedral supercages possesses an inner void of about 12 Å diameter and 8 triangular windows measuring 5−6 Å. As a result, more than 50% of the entire crystal volume is accessible to guest molecules despite the 2-fold interpenetration, judging from the Connolly surface with the probe radius of 1.4 Å. As we will show below, the overall framework of **SiMOF-11** is quite rigid and remains stable after complete evacuation.

SiMOF-12 is obtained when 2,6-naphthalenedicarboxylate (ndc) is used as the linker. In this structure, only one kind of SBU is observed, where 4 acetate groups on one side of the $[Si_8Zn_8]$ cluster are replaced by ndc (Figure 5a). Thus, the structural formula of **SiMOF-12** is $[(MeSiO_2)_8Zn_8(ndc)_2(OAc)_4]$. Many synthetic efforts have been made to replace all acetate groups with either ndc or mixed ndc−bdc linkers; however, no crystalline phase other than **SiMOF-12** was obtained. The SBU with 4 ndc linkers is interconnected in 4 alternating orientations to result in a tubular structure propagating along the c-axis of a tetragonal unit cell (Figure 5b). There are large openings on the side wall of the 1D tube, and $[Si_8Zn_8]$ clusters of other tubes reside in that space without

https://doi.org/10.1021/jacs.3c05950
J. Am. Chem. Soc. 2023, 145, 18598−18606

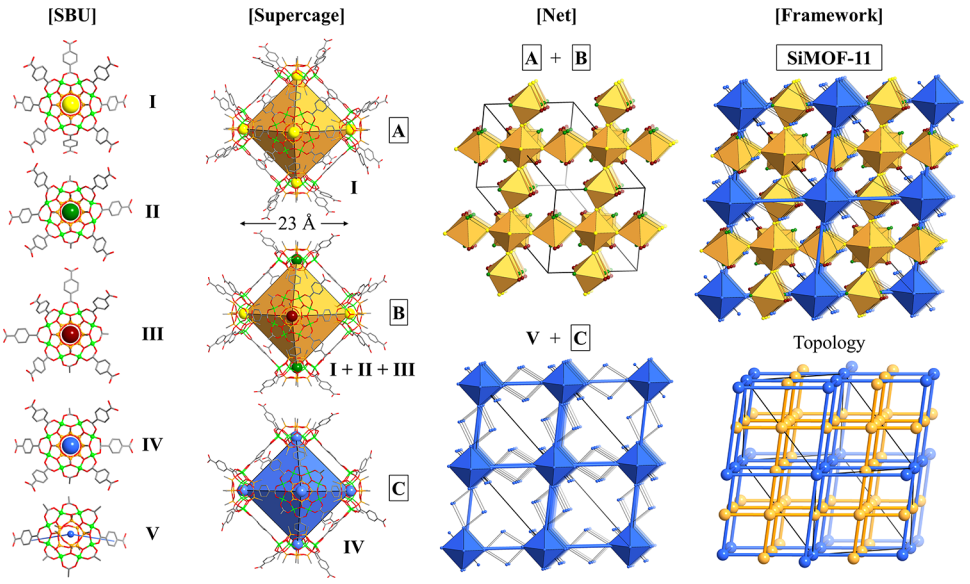

Figure 4. X-ray structure of **SiMOF-11** showing 5 unique SBUs, 3 independent supercages, and 2 interpenetrating nets built therefrom. All octahedral supercages possess accessible voids inside.

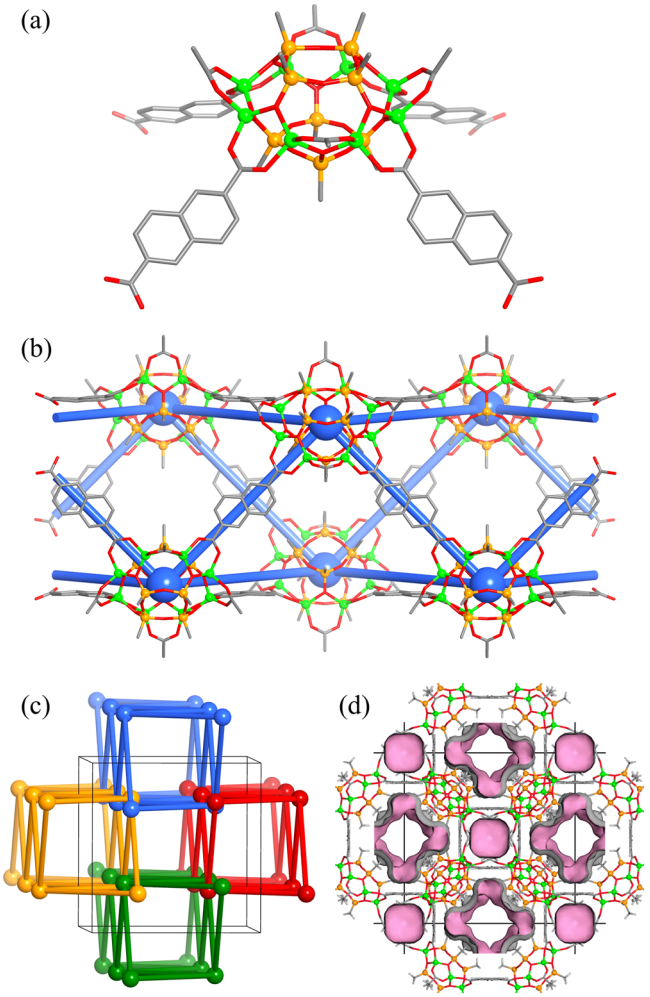

Figure 5. Structures of the SBU (a) and 1D tube (b) in **SiMOF-12**. (c) Simplified view showing 4 interdigitated tubes. (d) Connolly surface (probe radius 1.4 Å) of the framework showing 1D channels and isolated voids.

network entanglement. Therefore, the overall structure of **SiMOF-12** can be described as an interdigitated 3D net (Figure 5c). There are two kinds of voids in the structure, as shown in Figure 5d. Inside the tube lies a straight open channel with the smallest free passage of about 7 Å, and an isolated void measuring 5 Å in width and 12 Å in length is surrounded by 4 neighboring tubes.

The last structure to be described here is **SiMOF-21**, where the substituent on Si is a phenyl group and the linker is bdc. As shown by XRPD in Figure S2, **SiMOF-21** displays a structural change upon evacuation. The nature of this transition has been elucidated by determining single-crystal structures for both as-synthesized and evacuated crystals. According to the results, the bdc linkers in as-synthesized crystals are dynamically disordered because of DMF molecules coordinated to some Zn atoms (Figure S3). When the solvent molecules are removed, all of the bdc linkers in evacuated crystals show perfect ordering.

As a result of the released strain, the unit cell of **SiMOF-21** expands slightly along the *a*-axis (5% length) with a unit cell volume increase of about 2%. The bulk diffraction patterns measured in the presence of a solvent and after evacuation show good agreement with the simulations (Figure S2). In the structure of **SiMOF-21**, only one kind of SBU exists, and all 8 acetate groups of the $[Si_8Zn_8]$ cluster in **2** are replaced by bdc ligands, leading to the structural formula $[(PhSiO_2)_8Zn_8(bdc)_4]$ (Figure 6). The complete replacement of all 8 acetate ligands by 4 bdc linkers in **SiMOF-21** was somewhat surprising initially because, as we stated above, one kind of square antiprism vertex and one kind of linear edge are not expected to form together a well-defined 3D net. Further analysis of the high-quality single-crystal data reveals that the binding of some bdc linkers in the perfectly ordered, solvent-free structure still deviates significantly from the ideal linear coordination, resulting in considerable distortion of the nodal geometry from square antiprism. The full analysis of the topology underlying the net of **SiMOF-21** using TOPOS Pro[40] reveals that it is a uninodal 8-c net with the point symbol $\{3^6.4^{13}.5^9\}$, meaning that there are six 3-rings, thirteen 4-rings, and nine 5-rings around the node. The net is given the symbol **vcs** in the RCSR database[36] and has a transitivity of (1342). There are only a few known examples of

https://doi.org/10.1021/jacs.3c05950
J. Am. Chem. Soc. 2023, 145, 18598−18606

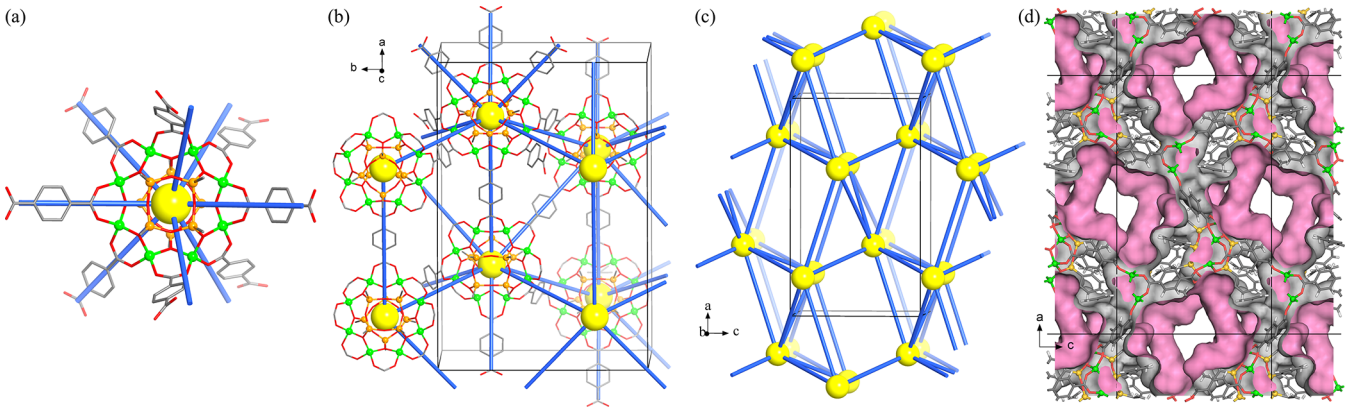

Figure 6. X-ray structure of **SiMOF-21** showing the SBU (a), partially expanded net (b), overall topology (c), and Connolly surface (1.4 Å) (d). Phenyl rings on the Si atom in (a) and (b) are omitted for clarity.

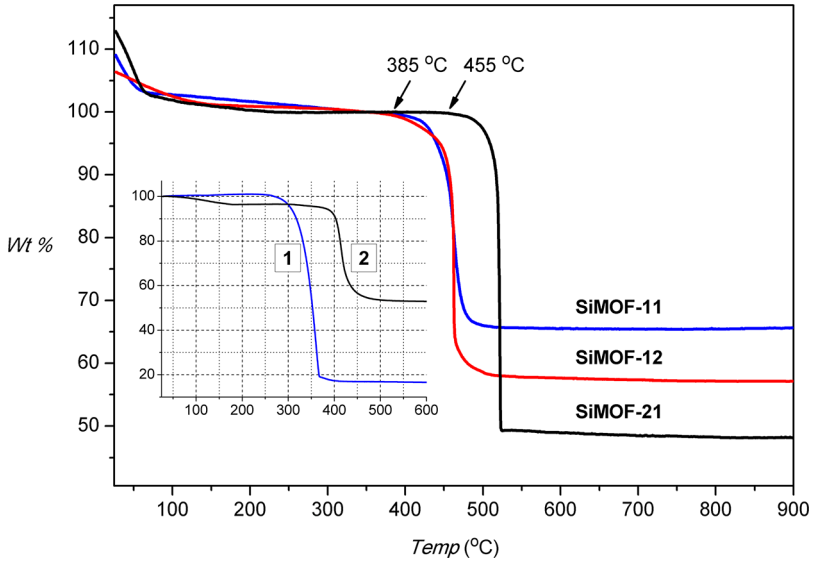

Figure 7. Thermogravimetric analysis of SiMOFs and clusters **1** and **2** (inset) measured under an O_2 environment. For SiMOFs, weights of samples are set to 100% after a complete removal of guests.

this net among metal−organic compounds.[41] Despite the complex network, the 3D net of **SiMOF-21** has 48% void volume in the form of interconnected and corrugated channels. The largest section of these three-dimensionally crosslinked voids measures about 12 × 9 Å^2 from the nearest van der Waals surface and is shown in Figure 6d.

Figure 7 compares the results of thermogravimetric analysis (TGA) for SiMOFs. Once volatile guests in the voids are removed from the solids at below 100 °C, all three frameworks display long plateaus before a clean, one-step decomposition of organic moieties occurs with an onset temperature of about 385 °C for **SiMOF-11** and **-12** and 455 °C for **SiMOF-21**. It can be said from the data that the thermal stabilities of all three SiMOFs are somewhat higher than those of typical carboxylate-based MOFs, where the decomposition of organic linkers starts at approximately 300 °C in most cases.[42] It also appears true that the network interpenetration or interdigitation seen in **SiMOF-11** and **-12** is not directly related to the higher stability because the single net of **SiMOF-21** shows even higher thermal stability than the other two. Rather, it should be the inherent stabilities of the SBUs that are directly responsible for the trends observed in TGA. As shown in the inset in Figure 7, the onset of thermal decay for **2** is about 100 °C higher than that for **1** for which thermal decay is accompanied by concomitant sublimation at about 270 °C or above.

The rigidity and stability of the open frameworks after removing all guest molecules are unequivocally proved by XRPD (Figure 8). Except for **SiMOF-21**, which shows a slight expansion as explained above, diffraction patterns for **SiMOF-11** and **-12** do not display a significant change upon thermal evacuation. The permanent porosity of all SiMOFs is shown by N_2 sorption isotherms (Figure 9). All three solids display characteristics of microporous materials, as expected, and **SiMOF-11** and **-21** possess a BET specific surface area greater than 1200 m^2/g (Figure S4). Total pore volumes measured at p/p_0 = 0.99 are 0.547, 0.215, and 0.494 cm^3/g for **SiMOF-11**, **-12**, and **-21**, respectively, and correspond to porosities of 54, 30, and 51%, respectively, based on crystallographic densities.

Another, probably more important, surface feature of SiMOFs is the fact that the pore surfaces are decorated mostly by methyl or phenyl groups on Si atoms because of the sandwich-type [$Si_4Zn_8Si_4$] structure of the SBUs. Consequently, all three SiMOFs synthesized here are deemed to possess hydrophobic surfaces, and this conjecture is proved true by a series of vapor sorption measurements. Figure 10 displays sorption isotherms for toluene, ethanol, methanol, and water vapors at 298 K. As

https://doi.org/10.1021/jacs.3c05950
J. Am. Chem. Soc. 2023, 145, 18598−18606

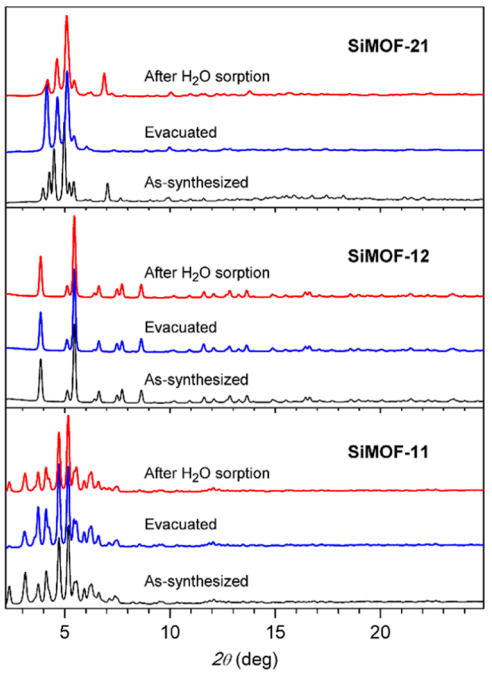

Figure 8. XRPD patterns for SiMOFs after evacuation and multiple cycles of H_2O adsorptions.

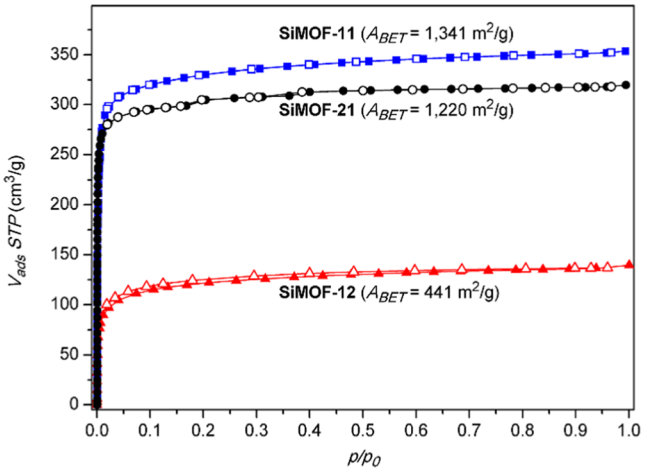

Figure 9. N_2 sorption isotherms at 77 K. Filled and open symbols denote adsorption and desorption, respectively.

shown clearly by the data in Figure 10a, voids in **SiMOF-11** can be saturated by vapors of all three organic solvents but a meaningful uptake of water vapor is not observed until the relative humidity reaches 90% or higher. Also shown is a clear trend that the adsorption of nonpolar toluene increases rapidly at very low p/p_0 (~0.01), while alcohols display breakthrough-like behavior with the breakthrough point sequentially delayed as the hydrophilicity increases to ethanol and then to methanol. The exclusion of water vapor and preferential uptake of hydrophobic guests by **SiMOF-11** closely resemble the reported behavior of the well-known hydrophobic MOF, ZIF-8.[43,44] Indeed, the total uptakes for toluene, ethanol, and methanol and their breakthrough pressures displayed by the two different MOFs are very similar, and not surprisingly, their specific surface areas are also comparable. A similar behavior is observed for **SiMOF-12** (Figure 10b), although the discrimination is less pronounced and total uptakes are lower. This is because the adsorption occurs inside 1D channels or isolated voids where overlapping potentials from opposite walls exhibit a strong affinity toward adsorptive molecules and slow down the diffusion. As shown in Figure 10c, **SiMOF-21** displays overall uptake values for organic vapors similar to those of **SiMOF-11** because the two possess comparable surface areas. The uptake pressure for methanol, however, is found to be slightly lower in **SiMOF-21**, implying a lower hydrophobicity of the surface. The adsorption of water vapor by **SiMOF-21** also begins at a lower humidity level (80%), and repeated adsorptions after reactivation show non-negligible uptakes. The subtle differences in the overall hydrophobic SiMOFs are further corroborated by measurements of water contact angles. As shown in Figure 10, **SiMOF-11** and **-12** are markedly more hydrophobic, with contact angles of 107(4) and 117(3)°, respectively, while **SiMOF-21** is borderline hydrophobic with 93(6)°. This behavior of **SiMOF-21** is probably because some Zn(II) ions in the SBU are accessible to solvent molecules, as shown in the X-ray structure of the as-synthesized **SiMOF-21** (Figure S3). Unlike other SiMOFs, the binding of carboxylate groups to Zn(II) ions in **SiMOF-21** are highly bent, and as a result, some of the tetrahedral metal atoms are open to solvent molecules with donor atoms.

The integrity of important chemical bonds in SiMOFs after thermal activation and repeated exposures to a high level of humidity have been evaluated by FT-IR spectroscopy (Figure S5). According to the results, strong IR bands representing ν(COO), ν(SiOSi), and ν(SiOZn) vibrations remain unchanged. The XRPD pattern in Figure 8 also shows that the

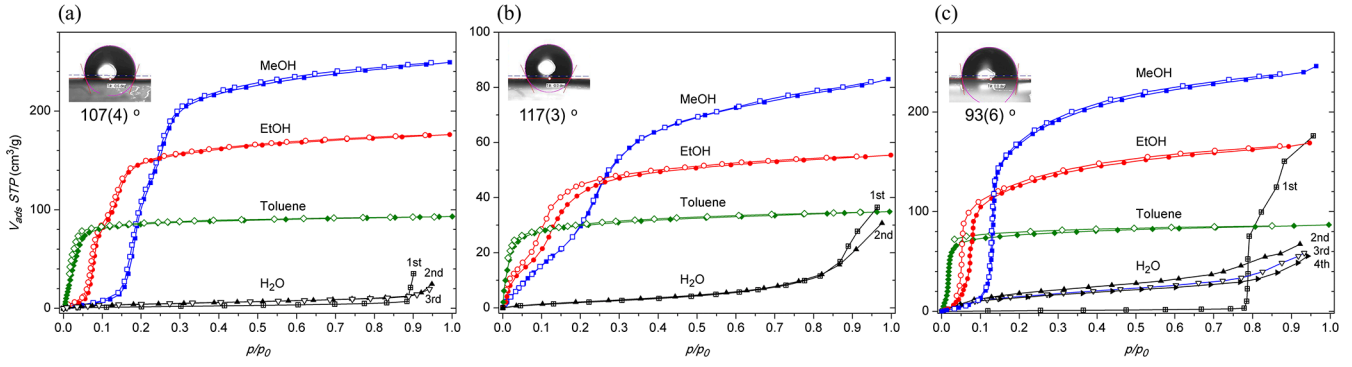

Figure 10. Vapor sorption isotherms for **SiMOF-11** (a), **-12** (b), and **-21** (c) at 298 K. H_2O adsorptions have been repeated until isotherm traces do not show significant changes. Images of water contact angles are shown as insets with the average values.

https://doi.org/10.1021/jacs.3c05950
J. Am. Chem. Soc. 2023, 145, 18598−18606

frameworks of **SiMOF-11** and **-12** are intact after multiple cycles of H_2O sorptions. The same applies true for the highly connected framework of **SiMOF-21**; however, some loss of long-range order cannot be ruled out, judging from the (200) diffraction at $2\theta = 4.2°$ showing a considerable decrease in intensity.

Hydrophobicity is often considered as a key property of MOFs for the separation of particular gases, volatile organic chemicals, and biphasic liquids, as well as for improving material stability under humid conditions.[45] Typical methods for enhancing the hydrophobicity of MOFs are post-synthetic treatments or ligand functionalization unless the framework is based on highly extended aromatic backbones.[46−48] The SiMOFs reported here suggest another and more convenient way of creating hydrophobic and highly porous solids without relying on post-synthetic or ligand modifications.[19] It would even be possible to modulate the hydrophobicity simply by choosing a Si precursor with different substituents.

Employing metal ions other than Zn(II) could also be a plausible and exciting attempt following this work. For example, 6-coordinate octahedral ions in place of Zn(II) in hydrophobic SiMOFs could create open metal sites in the framework for the preferential adsorption of CO_2 in humid air. Finally, establishing synthetic conditions for cyclic siloxanes of different nuclearities in the SBU would be truly impactful for future developments of SiMOFs. The occurrence of a tetrameric cycle is quite common in the literature, probably because of its thermodynamic stability.[49,50] However, there are abundant examples of other types of metal−siloxane clusters in the literature,[6−18] and thus, the synthetic strategy used in this work could be a useful guide for such efforts.

CONCLUSIONS

In conclusion, a facile and efficient pathway has been found to synthesize Zn(II)−siloxane clusters supported by carboxylate ligands. In this method, hydrolysis of alkoxysilane, condensation into a cyclic tetramer, coordination of Zn(II) ions, hydrolysis of carboxylate esters, and crosslinking of Zn−siloxane units into a crystal lattice all occur together in a one-pot solvothermal reaction. Depending on the carboxylate ligand, molecular clusters or 3D MOFs based on the same $[Si_8Zn_8]$ building block can be obtained. It is shown that all or a part of 8 carboxylate groups in the previously unknown SBU can be used to build thermally stable and porous frameworks, promising even more interesting discoveries with different ligands. The SiMOFs synthesized in this study are naturally hydrophobic as shown by water contact angles and a series of vapor sorption measurements; especially, **SiMOF-11** possesses a porosity and hydrophobicity comparable to those of ZIF-8. The observed surface features and stabilities against thermal and hydrolytic stresses are attributed to siloxane groups in the SBU, and thus, the synthetic approach for metal−siloxane clusters introduced here will be a valuable guide toward a new class of MOFs for practical applications.

ASSOCIATED CONTENT

Supporting Information

The Supporting Information is available free of charge at https://pubs.acs.org/doi/10.1021/jacs.3c05950.

Experimental details including synthesis and characterization, X-ray crystallography, list of large unit cell data, FT-IR spectra, XRPD patterns, and additional structural figures (PDF)

Accession Codes

CCDC 2267094−2267100 contain the supplementary crystallographic data for this paper. These data can be obtained free of charge via www.ccdc.cam.ac.uk/data_request/cif, or by emailing data_request@ccdc.cam.ac.uk, or by contacting The Cambridge Crystallographic Data Centre, 12 Union Road, Cambridge CB2 1EZ, UK; fax: +44 1223 336033.

AUTHOR INFORMATION

Corresponding Authors

Hyungphil Chun − *Department of Chemical and Molecular Engineering, Hanyang University, Ansan 15588, Republic of Korea;* orcid.org/0000-0003-2181-7469; Email: hchun@hanyang.ac.kr

Dohyun Moon − *Beamline Department, Pohang Accelerator Laboratory, Pohang 37673, Republic of Korea;* orcid.org/0000-0002-6903-0270; Email: dmoon@postech.ac.kr

Complete contact information is available at: https://pubs.acs.org/10.1021/jacs.3c05950

Funding

This work was supported by the National Research Foundation of Korea grant funded by the Korean Government (NRF-2022R1A2C1092102 to H.C. and NRF-2021R1A2C1003080 to D.M.).

Notes

The authors declare no competing financial interest.

ACKNOWLEDGMENTS

H.C. thanks the Pohang Accelerator Laboratory for beamline use (2023-1st-2D-007). The authors dedicate this paper to Prof. Myoung Soo Lah (UNIST, Korea) on the occasion of his 65th birthday.

REFERENCES

(1) Röshe, L.; John, P.; Reitmeier, R. Silicon Compounds, Organic. In *Ullmann's Encyclopedia of Industrial Chemistry*; John Wiley and Sons: San Francisco, 2003.

(2) Wolf, M. P.; Salieb-Beugelaar, G. B.; Hunziker, P. PDMS with designer functionalities—Properties, modifications strategies, and applications. *Prog. Polym. Sci.* **2018**, *83*, 97−134.

(3) Inagaki, S.; Guan, S.; Ohsuna, T.; Terasaki, O. An ordered mesoporous organosilica hybrid material with a crystal-like wall structure. *Nature* **2002**, *416*, 304−307.

(4) Fujita, S.; Inagaki, S. Self-Organization of Organosilica Solids with Molecular-Scale and Mesoscale Periodicities. *Chem. Mater.* **2008**, *20*, 891−908.

(5) Ovchinnikov, Y. E.; Shklover, V. E.; Struchkov, Y. T.; Levitsky, M. M.; Zhdanov, A. A. Synthesis and crystal structure of the salt $Na_6[(PhSiO_{1.5})_{22}Co_3O_6]\cdot 7H_2O$ containing a cobaltasiloxane anionic framework. *J. Organomet. Chem.* **1988**, *347*, 253−267.

(6) Astakhov, G. S.; Levitsky, M. M.; Zubavichus, Y. V.; Khrustalev, V. N.; Titov, A. A.; Dorovatovskii, P. V.; Smol'yakov, A. F.; Shubina, E. S.; Kirillova, M. V.; Kirillov, A. M.; Bilyachenko, A. N. Cu_6- and Cu_8-Cage Sil- and Germsesquioxanes: Synthetic and Structural Features, Oxidative Rearrangements, and Catalytic Activity. *Inorg. Chem.* **2021**, *60*, 8062−8074.

(7) Dankert, F.; von Hänisch, C. Siloxane Coordination Revisited: Si-O Bond Character, Reactivity and Magnificent Molecular Shapes. *Eur. J. Inorg. Chem.* **2021**, *2021*, 2907−2927.

(8) Liu, Y.-N.; Hou, J.-L.; Wang, Z.; Gupta, R. K.; Jagličić, Z.; Jagodič, M.; Wang, W.-G.; Tung, C.-H.; Sun, D. An Octanuclear Cobalt Cluster

Protected by Macrocyclic Ligand: In Situ Ligand-Transformation-Assisted Assembly and Single-Molecule Magnet Behavior. *Inorg. Chem.* **2020**, *59*, 5683−5693.
(9) Liu, Y.-N.; Su, H.-F.; Li, Y.-W.; Liu, Q.-Y.; Jagličić, Z.; Wang, W.-G.; Tung, C.-H.; Sun, D. Space Craft-like Octanuclear Co(II)-Silsesquioxane Nanocages: Synthesis, Structure, Magnetic Properties, Solution Behavior, and Catalytic Activity for Hydroboration of Ketones. *Inorg. Chem.* **2019**, *58*, 4574−4582.
(10) Bilyachenko, A. N.; Khrustalev, V. N.; Zubavichus, Y. V.; Vologzhanina, A. V.; Astakhov, G. S.; Gutsul, E. I.; Shubina, E. S.; Levitsky, M. M. High-Nuclearity (Cu_8-Based) Cage Silsesquioxanes: Synthesis and Structural Study. *Cryst. Growth Des.* **2018**, *18*, 2452−2457.
(11) Bilyachenko, A. N.; Yalymov, A. I.; Levitsky, M. M.; Korlyukov, A. A.; Es'kova, M. A.; Long, J.; Larionova, J.; Guari, Y.; Shul'pina, L. S.; Ikonnikov, N. S.; Trigub, A. L.; Zubavichus, Y. V.; Golub, I. E.; Shubina, E. S.; Shul'pin, G. B. First cage-like pentanuclear Co(II)-silsesquioxane. *Dalton Trans.* **2016**, *45*, 13663−13666.
(12) Bilyachenko, A. N.; Yalymov, A.; Dronova, M.; Korlyukov, A. A.; Vologzhanina, A. V.; Es'kova, M. A.; Long, J.; Larionova, J.; Guari, Y.; Dorovatovskii, P. V.; Shubina, E. S.; Levitsky, M. M. Family of Polynuclear Nickel Cagelike Phenylsilsesquioxanes; Features of Periodic Networks and Magnetic Properties. *Inorg. Chem.* **2017**, *56*, 12751−12763.
(13) Bilyachenko, A. N.; Dronova, M. S.; Yalymov, A. I.; Lamaty, F.; Bantreil, X.; Martinez, J.; Bizet, C.; Shul'pina, L. S.; Korlyukov, A. A.; Arkhipov, D. E.; Levitsky, M. M.; Shubina, E. S.; Kirillov, A. M.; Shul'pin, G. B. Cage-like Copper(II) Silsesquioxanes: Transmetalation Reactions and Structural, Quantum Chemical, and Catalytic Studies. *Chem. - Eur. J.* **2015**, *21*, 8758−8770.
(14) Shchegolikhina, O. I.; Pozdnyakova, Y. A.; Molodtsova, Y. A.; Korkin, S. D.; Bukalov, S. S.; Leites, L. A.; Lyssenko, K. A.; Peregudov, A. S.; Auner, N.; Katsoulis, D. E. Synthesis and Properties of Stereoregular Cyclic Polysilanols: *cis*-$[PhSi(O)OH]_4$, *cis*-$[PhSi(O)OH]_6$, and *Tris-cis-tris-trans*-$[PhSi(O)OH]_2$. *Inorg. Chem.* **2002**, *41*, 6892−6904.
(15) Hanssen, R. W. J. M.; Meetsma, A.; van Santen, R. A.; Abbenhuis, H. C. L. Synthesis, Structural Characterization, and Transmetalation Reactions of a Tetranuclear Magnesium Silsesquioxane Complex. *Inorg. Chem.* **2001**, *40*, 4049−4052.
(16) Kulakova, A. N.; Bilyachenko, A. N.; Levitsky, M. M.; Khrustalev, V. N.; Shubina, E. S.; Felix, G.; Mamontova, E.; Long, J.; Guari, Y.; Larionova, J. New Luminescent Tetranuclear Lanthanide-Based Silsesquioxane Cage-Like Architectures. *Chem. - Eur. J.* **2020**, *26*, 16594−16598.
(17) Veith, M.; Kolano, D.; Huch, V. Acid-Base Interactions of Pyrazine, Ethyl Acetate, Di-alcohols, and Lysine with the cyclic Alumosiloxane $(Ph_2SiO)_8[Al(O)OH]_4$ in View of Mimicking $Al_2O_3(H_2O)$ Surface Reactions. *Z. Anorg. Allg. Chem.* **2020**, *646*, 1846−1853.
(18) Hanssen, R. W. J. M.; van Santen, R. A.; Abbenhuis, H. C. L. The Dynamic Status Quo of Polyhedral Silsesquioxane Coordination Chemistry. *Eur. J. Inorg. Chem.* **2004**, *2004*, 675−683.
(19) Delmas, L. C.; White, A. J. P.; Pugh, D.; Evans, A.; Isbell, M. A.; Heng, J. Y. Y.; Lickiss, P. D.; Davies, R. P. Stable metal−organic frameworks with low water affinity built from methyl-siloxane linkers. *Chem. Commun.* **2020**, *56*, 7905−7908.
(20) Sanil, E. S.; Cho, K.-H.; Hong, D.-Y.; Lee, J. S.; Lee, S.-K.; Ryu, S. G.; Lee, H. W.; Chang, J.-S.; Hwang, Y. K. A polyhedral oligomeric silsesquioxane functionalized copper trimesate. *Chem. Commun.* **2015**, *51*, 8418−8420.
(21) Kataoka, S.; Banerjee, S.; Kawai, A.; Kamimura, Y.; Choi, J.-C.; Kodaira, T.; Sato, T.; Endo, A. Layered Hybrid Perovskites with Micropores Created by Alkylammonium Functional Silsesquioxane Interlayers. *J. Am. Chem. Soc.* **2015**, *137*, 4158−4163.
(22) Li, H.; Eddaoudi, M.; O'Keeffe, M.; Yaghi, O. M. Design and synthesis of an exceptionally stable and highly porous metal-organic framework. *Nature* **1999**, *402*, 276−279.
(23) Cavka, J. H.; Jakobsen, S.; Olsbye, U.; Guillou, N.; Lamberti, C.; Bordiga, S.; Lillerud, K. P. A New Zirconium Inorganic Building Brick Forming Metal Organic Frameworks with Exceptional Stability. *J. Am. Chem. Soc.* **2008**, *130*, 13850−13851.
(24) Chui, S. S.-Y.; Lo, S. M.-F.; Charmant, J. P. H.; Orpen, A. G.; Williams, I. D. A Chemically Functionalizable Nanoporous Material $[Cu_3(TMA)_2(H_2O)_3]_n$. *Science* **1999**, *283*, 1148.
(25) Ferey, G.; Mellot-Draznieks, C.; Serre, C.; Millange, F.; Dutour, J.; Surble, S.; Margiolaki, I. A Chromium Terephthalate−Based Solid with Unusually Large Pore Volumes and Surface Area. *Science* **2005**, *309*, 2040−2042.
(26) Huang, X.-C.; Lin, Y.-Y.; Zhang, J.-P.; Chen, X.-M. Ligand-Directed Strategy for Zeolite-Type Metal− Organic Frameworks: Zinc(ii) Imidazolates with Unusual Zeolitic Topologies. *Angew. Chem., Int. Ed.* **2006**, *45*, 1557−1559.
(27) Park, K. S.; Ni, Z.; Côté, A. P.; Choi, J. Y.; Huang, R.; Uribe-Romo, F. J.; Chae, H. K.; O'Keeffe, M.; Yaghi, O. M. Exceptional chemical and thermal stability of zeolitic imidazolate frameworks. *Proc. Natl. Acad. Sci. U.S.A.* **2006**, *103*, 10186−10191.
(28) Millot, Y.; Hervier, A.; Ayari, J.; Hmili, N.; Blanchard, J.; Boujday, S. Revisiting Alkoxysilane Assembly on Silica Surfaces: Grafting versus Homo-Condensation in Solution. *J. Am. Chem. Soc.* **2023**, *145*, 6671−6681.
(29) Władyczyn, A.; John, Ł. Unprecedented Route to Amide-Functionalized Double-Decker Silsesquioxanes Using Carboxylic Acid Derivatives and a Hydrochloride Salt of Aminopropyl-DDSQ. *Inorg. Chem.* **2023**, *62*, 5520−5530.
(30) Sato, N.; Kuroda, Y.; Wada, H.; Shimojima, A.; Kuroda, K. Preparation of Siloxane-Based Microporous Crystals from Hydrogen-Bonded Molecular Crystals of Cage Siloxanes. *Chem. - Eur. J.* **2018**, *24*, 17033−17038.
(31) Saito, S.; Wada, H.; Shimojima, A.; Kuroda, K. Synthesis of Zeolitic Macrocycles Using Site-Selective Condensation of Regioselectively Difunctionalized Cubic Siloxanes. *Inorg. Chem.* **2018**, *57*, 14686−14691.
(32) Chaikittisilp, W.; Kubo, M.; Moteki, T.; Sugawara-Narutaki, A.; Shimojima, A.; Okubo, T. Porous Siloxane-Organic Hybrid with Ultrahigh Surface Area through Simultaneous Polymerization-Destruction of Functionalized Cubic Siloxane Cages. *J. Am. Chem. Soc.* **2011**, *133*, 13832−13835.
(33) Chaikittisilp, W.; Sugawara, A.; Shimojima, A.; Okubo, T. Hybrid Porous Materials with High Surface Area Derived from Bromophenylethenyl-Functionalized Cubic Siloxane-Based Building Units. *Chem. - Eur. J.* **2010**, *16*, 6006−6014.
(34) Lim, D.-W.; Lee, H.; Kim, S.; Cho, I. H.; Yoon, M.; Choi, Y. N. An unprecedented single platform via cross-linking of zeolite and MOFs. *Chem. Commun.* **2016**, *52*, 6773−6776.
(35) Yuan, N.; Zhang, X.; Wang, L. The marriage of metal−organic frameworks and silica materials for advanced applications. *Coord. Chem. Rev.* **2020**, *421*, No. 213442.
(36) O'Keeffe, M.; Peskov, M. A.; Ramsden, S. J.; Yaghi, O. M. The Reticular Chemistry Structure Resource (RCSR) Database of, and Symbols for, Crystal Nets. *Acc. Chem. Res.* **2008**, *41*, 1782−1789.
(37) A locally written Python script was used to analyze CIF data obtained from CSD v. 5.44 (https://www.ccdc.cam.ac.uk/solutions/software/csd/).
(38) The largest volume for a non-cubic unit cell before this work is 257,127 $Å^3$ in $R\bar{3}m$: Bar, A. K.; Chakrabarty, R.; Mostafa, G.; Mukherjee, P. S. Self-Assembly of a Nanoscopic $Pt_{12}Fe_{12}$ Heterometallic Open Molecular Box Containing Six Porphyrin Walls. *Angew. Chem., Int. Ed.* **2008**, *47*, 8455−8459.
(39) Lu, Z.; Du, L.; Guo, R.; Zhang, G.; Duan, J.; Zhang, J.; Han, L.; Bai, J.; Hupp, J. T. Double-Walled $Zn_{36}@Zn_{104}$ Multicomponent Senary Metal−Organic Polyhedral Framework and Its Isoreticular Evolution. *J. Am. Chem. Soc.* **2021**, *143*, 17942−17946.
(40) Blatov, V. A.; Shevchenko, A. P.; Proserpio, D. M. Applied Topological Analysis of Crystal Structures with the Program Package ToposPro. *Cryst. Growth Des.* **2014**, *14*, 3576−3586.

https://doi.org/10.1021/jacs.3c05950
J. Am. Chem. Soc. 2023, 145, 18598−18606

(41) Occurrence of **vcs** net in *The Samara Topological Data Center*. https://topcryst.com/topology/vcs (accessed July 19, 2023).
(42) Healy, C.; Patil, K. M.; Wilson, B. H.; Hermanspahn, L.; Harvey-Reid, N. C.; Howard, B. I.; Kleinjan, C.; Kolien, J.; Payet, F.; Telfer, S. G.; Kruger, P. E.; Bennett, T. D. The thermal stability of metal-organic frameworks. *Coord. Chem. Rev.* **2020**, *419*, No. 213388.
(43) Hunter-Sellars, E.; Saenz-Cavazos, P. A.; Houghton, A. R.; McIntyre, S. R.; Parkin, I. P.; Williams, D. R. Sol−Gel Synthesis of High-Density Zeolitic Imidazolate Framework Monoliths via Ligand Assisted Methods: Exceptional Porosity, Hydrophobicity, and Applications in Vapor Adsorption. *Adv. Funct. Mater.* **2020**, No. 2008357.
(44) Zhang, K.; Lively, R. P.; Dose, M. E.; Brown, A. J.; Zhang, C.; Chung, J.; Nair, S.; Koros, W. J.; Chance, R. R. Alcohol and water adsorption in zeolitic imidazolate frameworks. *Chem. Commun.* **2013**, *49*, 3245−3247.
(45) Jayaramulu, K.; Geyer, F.; Schneemann, A.; Kment, Š.; Otyepka, M.; Zboril, R.; Vollmer, D.; Fischer, R. A. Hydrophobic Metal−Organic Frameworks. *Adv. Mater.* **2019**, *31*, No. 1900820.
(46) Lee, S.-K..; Lee, Y. J.; Cho, K.; Lee, U-H.; Chang, J.-S. A Fluorinated Metal-Organic Framework, FMOF-2, for Preferential Adsorption of Ethane over Ethylene. *Bull. Korean Chem. Soc.* **2021**, *42*, 286−289.
(47) Yang, S.; Peng, L.; Sun, D. T.; Asgari, M.; Oveisi, E.; Trukhina, O.; Bulut, S.; Jamali, A.; Queen, W. L. A new post-synthetic polymerization strategy makes metal−organic frameworks more stable. *Chem. Sci.* **2019**, *10*, 4542−4549.
(48) Rao, K. P.; Higuchi, M.; Sumida, K.; Furukawa, S.; Duan, J.; Kitagawa, S. Design of Superhydrophobic Porous Coordination Polymers through the Introduction of External Surface Corrugation by the Use of an Aromatic Hydrocarbon Building Unit. *Angew. Chem., Int. Ed.* **2014**, *53*, 8225−8230.
(49) Liu, Y.; Chaiprasert, T.; Ouali, A.; Unno, M. Well-defined cyclic silanol derivatives. *Dalton Trans.* **2022**, *51*, 4227−4245.
(50) Kudo, T.; Gordon, M. S. Theoretical Studies of the Mechanism for the Synthesis of Silsesquioxanes. 2. Cyclosiloxanes (D_3 and D_4). *J. Phys. Chem. A* **2000**, *104*, 4058−4063.

https://doi.org/10.1021/jacs.3c05950
J. Am. Chem. Soc. 2023, 145, 18598−18606